

This article is published as part of the *Dalton Transactions* themed issue entitled:

Dalton Discussion 12: Catalytic C-H and C-X Bond Activation

Published in [issue 43, 2010](#) of *Dalton Transactions*

Read about the Dalton Discussion 12 meeting on the [Dalton Transactions Blog](#)

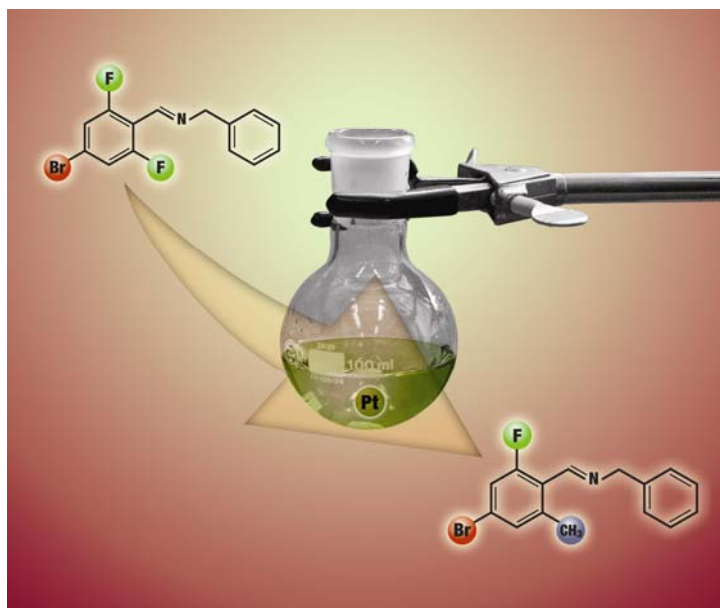


Image reproduced with the permission of Jennifer Love

Articles in the issue include:

PERSPECTIVES:

[Arylation of unactivated arenes](#)

Aiwen Lei, Wei Liu, Chao Liu and Mao Chen
Dalton Trans., 2010, DOI: 10.1039/C0DT00486C

[The mechanism of the modified Ullmann reaction](#)

Elena Sperotto, Gerard P. M. van Klink, Gerard van Koten and Johannes G. de Vries
Dalton Trans., 2010, DOI: 10.1039/C0DT00674B

[Cross coupling reactions of polyfluoroarenes via C–F activation](#)

Alex D. Sun and Jennifer A. Love
Dalton Trans., 2010, DOI: 10.1039/C0DT00540A

HOT ARTICLE:

[The unexpected role of pyridine-2-carboxylic acid in manganese based oxidation catalysis with pyridin-2-yl based ligands](#)

Dirk Pijper, Pattama Saisaha, Johannes W. de Boer, Rob Hoen, Christian Smit, Auke Meetsma, Ronald Hage, Ruben P. van Summeren, Paul L. Alsters, Ben L. Feringa and Wesley R. Browne
Dalton Trans., 2010, DOI: 10.1039/C0DT00452A

Visit the *Dalton Transactions* website for more cutting-edge inorganic and organometallic research
www.rsc.org/dalton

Alkyne insertion into cyclometallated pyrazole and imine complexes of iridium, rhodium and ruthenium; relevance to catalytic formation of carbo- and heterocycles†

Youcef Boutadla, David L. Davies,* Omar Al-Duaij, John Fawcett, Rachel C. Jones and Kuldip Singh

Received 9th April 2010, Accepted 25th May 2010

DOI: 10.1039/c0dt00280a

The cyclometallated complexes $[MCl(C^{\wedge}N)(ring)]$ ($HC^{\wedge}N$ = 2-phenylpyrazole, M = Ir, Rh ring = Cp^* ; M = Ru, ring = p -cymene) readily undergo insertion reactions with $RC\equiv CR$ (R = CO_2Me , Ph) to give mono insertion products, the rhodium complex also reacts with $PhC\equiv CH$ regioselectively to give an analogous product. The products of the reactions of the cyclometallated imine complexes $[MCl(C^{\wedge}N)Cp^*]$ ($HC^{\wedge}N$ = $PhCH=NR$, R = Ph, CH_2CH_2OMe , Me; M = Ir, Rh) with $PhC\equiv CPh$ depend on the substituent R ; when R = CH_2CH_2OMe a monoinsertion is observed, however for R = Me the initial insertion product is unstable, undergoing reductive elimination with loss of the organic fragment, and for R = Ph no metal-containing product is isolated. With $PhC\equiv CH$ the cyclometallated imine complexes can give mono or di-insertion products. The implications for catalytic synthesis of carbo- and heterocycles by a tandem C–H activation, alkyne insertion mechanism are discussed.

Introduction

Cyclometallation reactions in which a C–H bond is converted to an M–C bond have been known for decades. Recently there has been renewed interest in these reactions because of the wide applications of cyclometallated complexes.¹ In 2003 we noted that acetate-assisted cyclometallation of various N-donor groups occurred under very mild conditions with $[MCl_2Cp^*]_2$ (M = Ir, Rh) or $[RuCl_2(p\text{-cymene})]_2$.² Subsequent studies by us³ and others⁴ have shown that these are ambiphilic metal ligand activations (AMLA),⁵ involving an electrophilic metal centre with assistance by hydrogen bonding to the free arm of a coordinated acetate. Since our initial publication this AMLA methodology has also been extended to other donor groups.^{6–8} Therefore, this method constitutes a facile high yield route to a range of half sandwich cyclometallated complexes and hence provides an opportunity to study their reactivity.

In recent years there has been substantial progress in incorporating a C–H activation step, usually cyclometallation, and subsequent C–C bond formation into catalytic cycles.⁹ Such processes, may remove the need to prepare halogenated precursors for further functionalisation, hence provide a cheaper and more atom-economic methodology. Coupling a C–H bond activation step with an alkyne or alkene insertion into the cyclometallated M–C bond and subsequent reductive elimination is a potential route to heterocyclic products. Miura and coworkers have recently reported a number of reactions to form carbocycles or heterocycles

catalysed by $[MCl_2Cp^*]_2$ (M = Ir, Rh) in which they propose that cyclometallation at Cp^*M followed by alkyne insertion into the M–C bond are important steps in the catalytic cycle.^{10–12} A similar sequence is likely involved in Cp^*Rh catalysed synthesis of indoles¹³ and isoquinolines¹⁴ reported by Fagnou's group. At the moment very little is known about the scope of these reactions, in terms of the directing groups that can be used in the initial cyclometallation and the range of substituents that can be used on the alkyne. In this regard studies of the cyclometallation reaction and subsequent reactions of the cyclometallated complexes with alkynes are important to understand selectivity and reactivity issues in the catalytic processes.

The reactivity of half-sandwich cyclometallated complexes with unsaturated substrates is, comparatively little studied. Early work by Pfeffer *et al.* showed that arene ruthenium cyclometallated complexes $[RuCl(DMBA)(arene)]$ ($DMBAH$ = dimethylbenzylamine) would react with alkynes to form coordinated isoquinolinium salts which could be liberated from the metal using copper salts as oxidants.¹⁵ Recently Jones *et al.* showed that related Cp^*Rh and Cp^*Ir cyclometallated imine and pyridine complexes undergo alkyne insertion with DMAD (dimethylacetylene dicarboxylate); oxidative coupling of the pyridine complex with $CuCl_2$ generated isoquinolinium salts *via* C–N reductive elimination, however this only occurred for the rhodium complex not iridium.⁷ In contrast Fagnou provided evidence to suggest that, in some cases at least, C–N reductive elimination can occur before oxidation by copper salts.¹⁴ Miura *et al.* have also reported examples of C–C reductive elimination after alkyne insertion, to give carbocycles.¹²

It is clear from these studies that the nature of the directing group, the metal, and the alkyne substituents can all have a major impact on the outcome of the reactions. We recently reported our studies of alkyne insertion reactions with cyclometallated oxazolines.¹⁶ Here we extend those results to reactions of cyclometallated pyrazoles and imines and comment on their relevance to

Department of Chemistry, University of Leicester, Leicester, U.K., LE1 7RH. E-mail: dld3@le.ac.uk

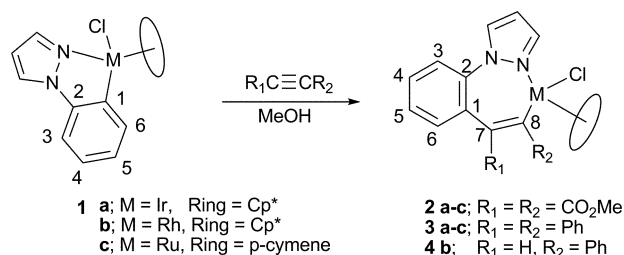
† Based on the presentation given at Dalton Discussion No. 12, 13–15th September 2010, Durham University, UK.

‡ Electronic supplementary information (ESI) available: Figures showing structures of **3b,c** and Table of crystallographic data for **3b,c**. CCDC reference numbers 772790–772800. For ESI and crystallographic data in CIF or other electronic format see DOI: 10.1039/c0dt00280a

the catalytic formation of heterocycles reported by Miura^{10–12} and Fagnou.^{13,14}

Results and discussion

Complexes **1a–c** were prepared by acetate assisted cyclometallation of 2-phenylpyrazole with $[\text{MCl}_2\text{Cp}^*]_2$ ($\text{M} = \text{Ir}, \text{Rh}$) or $[\text{RuCl}_2(p\text{-cymene})]_2$. Full characterisation of these products is described elsewhere.¹⁷ The reactions of **1a–c** with alkynes were then investigated (Scheme 1).



Scheme 1

Reaction of **1a–c** with DMAD in MeOH led to monoinsertion products **2a–c** in good yields. The ^1H NMR spectra of **2a–c** show the expected signals for the cyclometallated phenylpyrazole and two methoxy signals for the inequivalent CO_2Me groups of the alkyne. The Cp^* signals in **2a,b** occur at *ca.* δ 1.3, about 0.3 ppm to higher field than the corresponding starting complexes. This can be explained by a ring-current effect of the Cp^* lying over the original cyclometallated phenyl ring of the phenylpyrazole (see X ray structure below). Similar ring current effects have been observed for cyclometallated bisoxazoline benzene complexes,¹⁸ and related complexes formed by alkyne insertion into Cp^*M cyclometallated complexes.^{7,16} The ^1H NMR spectrum of **2c** also shows evidence for a ring current affecting the four aromatic protons of *p*-cymene which are 0.03–0.95 ppm upfield from the corresponding signals in **1c**. The inequivalence of these four aromatic protons is consistent with the metal centre being chiral and epimerisation being slow on the NMR timescale.

Complexes **2a,b,c** have been characterised by X-ray crystallography and the structures are shown in Fig. 1 with selected bond distances and angles. The structures confirm that the alkyne

has inserted into the $\text{M}-\text{C}$ bond rather than the $\text{M}-\text{N}$ bond, to form a seven-membered ring, as found in related alkyne insertions into cyclometallated imine, pyridine and oxazoline half-sandwich complexes.^{7,16} However, no ring closure by C,N bond formation has occurred, in contrast to observations by Pfeffer *et al.* on reactions of alkynes with cyclometallated amine complexes $[\text{RuCl}(\text{DMBA})(\text{arene})]$.¹⁵ It is noticeable that the Cp^* in **2a,b**, and the *p*-cymene in **2c**, lie over the originally cyclometallated phenyl rings consistent with the ring current effects discussed above. The geometry around the metal is very similar in the three complexes and to complexes formed by insertion of DMAD into $[\text{MCl}(\text{C}^*\text{N})\text{Cp}^*]$ ($\text{M} = \text{Rh}, \text{Ir}$ $\text{HC}^*\text{N} = \text{phenylpyridine}$) reported by Jones *et al.*⁷ The $\text{M}-\text{C}$ bond length is slightly shorter than the $\text{M}-\text{N}$ in each complex. The chelate angles $\text{C}(1)-\text{M}-\text{N}(1)$ for the seven membered rings range from $83.35(16)^\circ$ in **2c** to $85.67(9)^\circ$ in **2b** which are considerably larger than those for five membered rings in **1a–c** [range $77.4(1)$ to $78.5(3)^\circ$].¹⁷ The formation of the seven-membered ring also requires a non-planar arrangement of the phenyl and pyrazole rings. Thus in **2a–c** the angle between the mean least squares plane of the phenyl and pyrazole varies between 51.35 (**2b**) and 54.52° (**2c**), whilst in the five-membered ring precursors **1a–c** the corresponding angle varies between only 3.42° (**1c**) and 5.05° (**1b**).¹⁷

Similar reactions of **1a–c** with $\text{PhC}\equiv\text{CPh}$ in MeOH proceeded in 1–3 h, to give products **3a–c** in moderate to good yields. As found for **2a,b**, the ^1H NMR spectra of **3a,b** show the Cp^* signals approximately 0.30 ppm upfield compared to **1a,b** as expected for the seven-membered ring insertion product. The pyrazole signals are at similar chemical shifts to those observed for **2a,b**. The ^1H NMR spectrum of ruthenium complex **3c** is similar to those of **3a,b** except with signals for a *p*-cymene replacing those for Cp^* . Notably, the isopropyl group gives rise to two doublets (at δ 1.08 and 1.23) and the four aromatic protons of the *p*-cymene are also inequivalent, giving four doublets of doublets between δ 3.48 and 5.54, again showing upfield shifts (0.01 to 1.59 ppm) in comparison to the starting complex **1c** due to the ring current effect described above. These data are also consistent with the metal centre being chiral and epimerisation being slow on the NMR timescale. The ^{13}C NMR spectra of **3a–c** show the expected number of $\text{C}-\text{H}$ and quaternary carbons, the metallated carbons (C^{11}) being observed between 15 and 6 ppm to higher field than in **2a–c**.

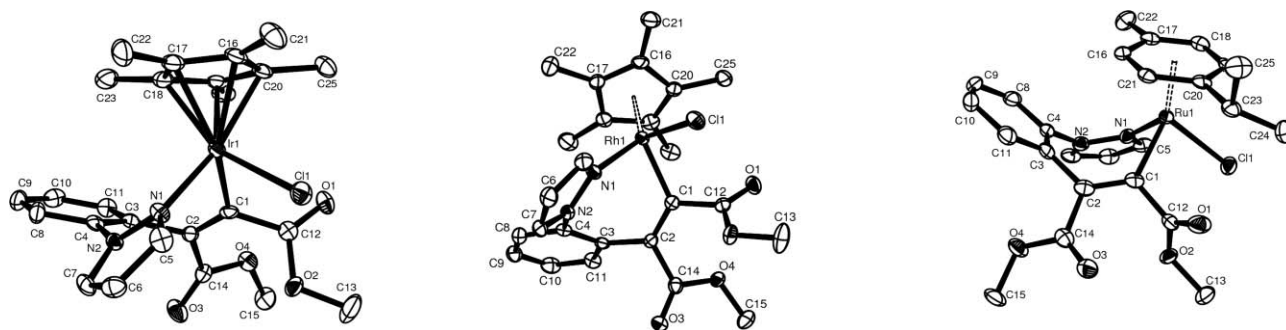


Fig. 1 Molecular structure and atom numbering scheme for (a) **2a**, (b) **2b**, (c) **2c** with 50% displacement ellipsoids, all H atoms are omitted for clarity. Selected bond distances (Å) and angles ($^\circ$) For **2a**: $\text{Ir}-\text{N}(1)$ 2.086(4), $\text{Ir}-\text{C}(1)$ 2.050(5), $\text{Ir}-\text{Cl}(1)$ 2.4183(12), $\text{C}(1)-\text{Ir}-\text{N}(1)$ 85.08(16), $\text{C}(1)-\text{Ir}-\text{Cl}(1)$ 88.51(13), $\text{N}(1)-\text{Ir}-\text{Cl}(1)$ 86.84(11). For **2b**: $\text{Rh}-\text{C}(1)$ 2.040(3), $\text{Rh}-\text{N}(1)$ 2.093(2), $\text{Rh}-\text{Cl}(1)$ 2.4131(7), $\text{C}(1)-\text{Rh}-\text{N}(1)$ 85.67(9), $\text{C}(1)-\text{Rh}-\text{Cl}(1)$ 89.92(8), $\text{N}(1)-\text{Rh}-\text{Cl}(1)$ 88.61(6). For **2c**: $\text{Ru}-\text{C}(1)$ 2.070(4), $\text{Ru}-\text{N}(1)$ 2.097(4), $\text{Ru}-\text{Cl}(1)$ 2.4183(17), $\text{C}(1)-\text{Ru}-\text{N}(1)$ 83.35(16), $\text{C}(1)-\text{Ru}-\text{Cl}(1)$ 89.37(14), $\text{N}(1)-\text{Ru}-\text{Cl}(1)$ 85.94(11).

Complexes **3a–c** were also characterised by X-ray crystallography and the structure of **3a** is shown in Fig. 2 with selected bond distances and angles. The structures of **3b** and **3c** are in the supplementary material.† **3c** has two molecules in the unit cell and the Ru—C and Ru—N bond lengths vary in the two molecules therefore bond lengths and angles are not discussed below. Complexes **3a–c** have similar structures to **2a–c** and confirm that the alkyne has inserted into the M—C bond rather than the M—N bond, to form a seven-membered ring. The M—C bond lengths of **3a,b** [2.069(6) and 2.061(7) Å respectively] are shorter than the M—N distances [2.088(5) and 2.096(6) Å respectively] as found in **2a,b**. However the M—C bond lengths of **3a,b** are longer than those of **2a,b** whilst the M—N bond lengths are unchanged. There are some small changes in the bond angles of **3a,b** compared to **2a,b**, the chelate angles decrease slightly while the C(1)—M—Cl(1) angles increase slightly. This is presumably due to the increased size of the phenyl substituent on C(1) in **3a,b** compared with CO₂Me in **2a,b**. As found in **2a–c** the phenyl and pyrazole are not coplanar, the angles between the planes of the pyrazole and original cyclometallated phenyl are 52.66° and 45.55° in **3a** and **3b** respectively.

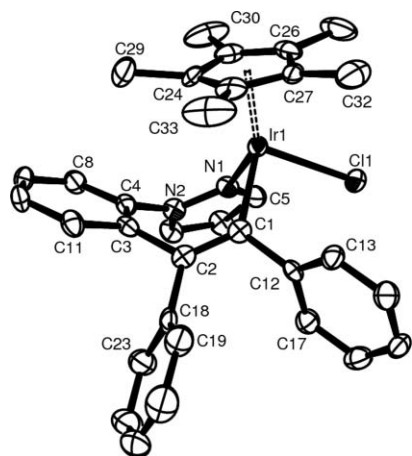


Fig. 2 Molecular structure and atom numbering scheme for **3a** with 50% displacement ellipsoids, all H atoms are omitted for clarity. Selected bond distances (Å) and angles (°): Ir—N(1) 2.088(5), Ir—C(1) 2.069(6), Ir—Cl(1) 2.4254(15), C(1)—Ir—N(1) 82.9(2), C(1)—Ir—Cl(1) 89.67(16), N(1)—Ir—Cl(1) 86.45(14).

The cyclometallation of 2-phenylpyrazole to form **1a–c** and subsequent reaction of these complexes with disubstituted alkynes to form complexes **2** and **3** demonstrates that the first two steps of the mechanism postulated by Miura for catalytic formation of naphthylazoles, namely C—H activation and alkyne insertion,¹² are entirely feasible. (Note, the catalysis occurs at 80 °C whilst the cyclometallation and alkyne insertion both occur at room temperature.)

Miura's catalytic reactions all involve disubstituted alkynes. Indeed, there are very few reported cases of alkyne insertions involving monosubstituted alkynes.¹⁹ The only examples of stoichiometric reactions of a half-sandwich cyclometallated complex with terminal alkynes are with [CoI(DMBA)(Cp)] which only reacts with terminal alkynes,²⁰ and our results for a Cp*Ir cyclometallated oxazoline complex which reacts with PhC≡CH to give either a monoinserted product or a diinsertion depending

on the exact precursor and reaction conditions used.¹⁶ Hence the reaction of **1a,b** with PhC≡CH was attempted.

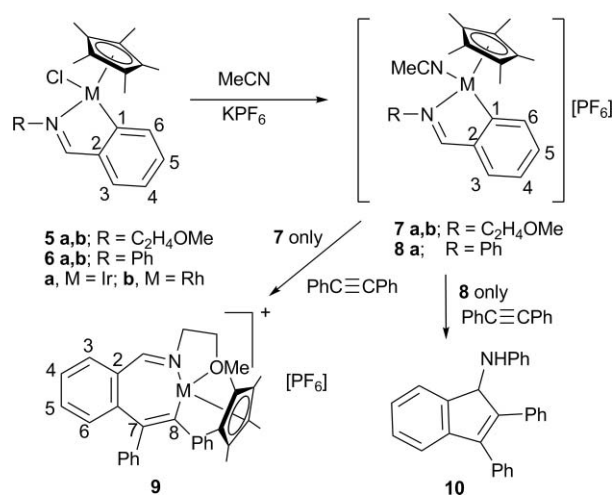
The reaction of Ir complex **1a** with PhC≡CH in MeOH was monitored by ES-MS and after 5 min, three signals were observed at *m/z* 471, 573 and 675 which were assigned as [**1a** – Cl], [**1a** – Cl + PhCCH] and [**1a** – Cl + 2 PhCCH] respectively. The reaction appears to give a mixture of mono and diinsertion products with the second insertion occurring at a similar rate to the first one, so that it is not possible to get clean conversion into the monoinserted product. This is similar to what we found with an oxazoline complex.¹⁶ Addition of another equivalent of PhC≡CH led to more of the diinsertion product but still gave a mixture which we were unable to separate.

The corresponding reaction of PhC≡CH with **1b** was complete after 2 h; the ES-MS showed only one product peak at *m/z* 483 [**1b** – Cl + PhCCH]. This suggests that the first and the second insertions are slower for rhodium than iridium, such that the monoinserted product can be isolated. The ¹H NMR spectrum shows one set of signals with a 1 : 1 : 1 ratio of Cp* to the cyclometallated phenylpyrazole and PhC≡CH which suggests only one regioisomer was obtained. The Cp* signal is observed upfield from **1b** at δ 1.30, (c.f. δ 1.35 in **3b**). In the ¹³C NMR spectrum, the expected number of quaternary and C—H carbons for one insertion of PhC≡CH is seen. The metallated carbon is easily identified due to coupling with rhodium and is observed as a doublet (*J* 125 Hz) at δ 178.64. A DEPT spectrum showed that the metallated C is a quaternary carbon which allows us to assign the product as **4b** having the phenyl substituent, rather than the hydrogen, next to the metal. This regioselectivity is identical to that observed for a Cp*Ir cyclometallated oxazoline complex.¹⁶

The reaction of PhC≡CH with cycloruthenated complex **1c** was also investigated. After 1 h the ES-MS showed one peak at *m/z* 481 [**1c** – Cl + PhCCH], however the ¹H NMR spectrum of this sample showed three sets of *p*-cymene signals, one of which was assigned to the starting complex. To try to convert more of the starting complex into product another equivalent of PhC≡CH was added to the NMR sample. Unfortunately, instead of leading to more conversion, decomposition occurred, the ¹H NMR spectrum showed broad signals and liberation of free *p*-cymene.

In none of the above reactions does C,N bond formation occur spontaneously in the alkyne insertion products **2a–c**, **3a–c** or **4b**. Jones showed that with pyridine or an imine as a directing group for the initial cyclometallation, oxidation of the alkyne insertion products with copper(II) salts can induce C,N bond formation.⁷ Reaction of **2b** with Cu(OAc)₂ was attempted but at room temperature there was no reaction. This is not surprising since no C,N bond formation is observed by Miura in the use of pyrazole as a directing group in catalytic synthesis of naphthalenes and these reactions occur at 80 °C.¹²

To investigate further the effects of the donor group on reactivity we have studied some reactions of cyclometallated imines (Scheme 2). As we found for half-sandwich cyclometallated oxazoline complexes, and as observed previously for palladium complexes,^{21,22} reactions with alkynes were facilitated by substituting the chloride in the starting complexes with acetonitrile to provide cationic complexes.¹⁶ Stirring complexes **5a,b** or **6a** overnight in acetonitrile in the presence of KPF₆ gave cationic complexes **7a,b** and **8a** respectively. The ¹H NMR spectra show, in addition to signals for the cyclometallated ligand and Cp*, a singlet integrating to



Scheme 2

3 protons at δ 2.36, 2.23 and 2.49 for **7a,b** and **8a** respectively assigned to coordinated NCMe, (free NCMe is observed at δ 2.00). The CH₂O protons of **7a,b** give rise to two multiplets, the inequivalence, suggesting that epimerisation at the metal is slow on the NMR timescale unlike an analogous iridium cyclometallated oxazoline complex which was fluxional on the NMR timescale.¹⁶

Complexes **7b** and **8a** were characterised by X-ray crystallography and the structures are shown in Fig. 3 and 4 respectively with selected bond distances and angles. The complexes adopt the expected pseudo-octahedral structure with the Cp* ligand occupying three facial coordination sites of the metal and confirms the coordination of NCMe. As found in other cyclometallated complexes,^{2,8} both complexes show two long [2.240(3) to 2.273(3) Å] and three short [2.138(3) to 2.172(3) Å] M—C bonds to the Cp*, with the longer ones approximately *trans* to the metallated carbon. The M—N(imine) bond lengths [2.090(3) and 2.095(2) Å] in **7b** and **8a** are longer than the M—N(NCMe) [2.069(3) and 2.044(3) Å respectively] consistent with

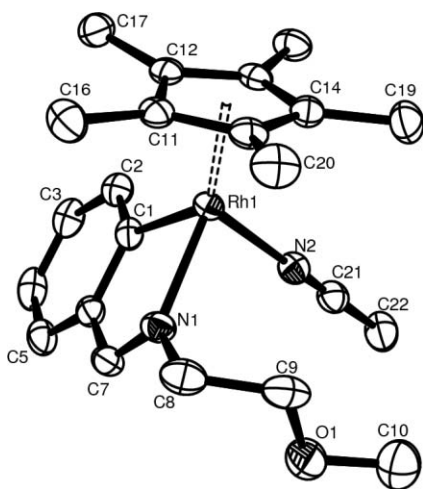


Fig. 3 Molecular structure and atom numbering scheme for the cation of **7b** with 50% displacement ellipsoids, all H atoms are omitted for clarity. Selected bond distances (Å) and angles (°): Rh—C(1) 2.032(3), Rh—N(1) 2.090(3), Rh—N(2) 2.069(3), C(1)—Rh—N(1) 78.54(11), C(1)—Rh—N(2) 83.80(11), N(1)—Rh—N(2) 89.74(10).

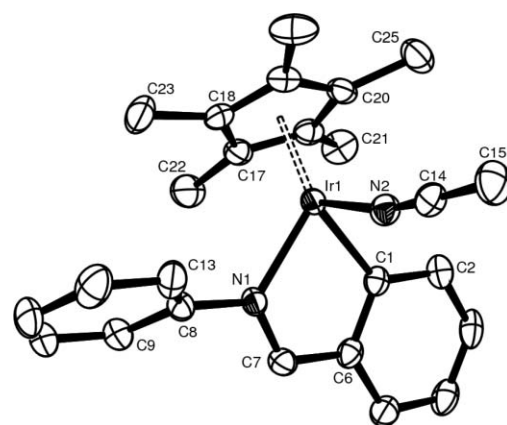


Fig. 4 Molecular structure and atom numbering scheme for the cation of **8a** with 50% displacement ellipsoids, all H atoms are omitted for clarity. Selected bond distances (Å) and angles (°): Ir(1)—N(2) 2.044(3), Ir(1)—C(1) 2.048(3), Ir(1)—N(1) 2.095(2), N(2)—Ir(1)—C(1) 87.57(11), N(2)—Ir(1)—N(1) 92.29(10), C(1)—Ir(1)—N(1) 77.52(11).

bonds to an sp² rather than an sp nitrogen. The phenyl substituent on nitrogen in **8a** is rotated out of the plane of the cyclometallated fragment (dihedral angle C(7)—N(1)—C(8)—C(9) = 122.8°) and is approximately parallel to the Cp* (angle between least squares planes = 6.4°).

Reactions of the cationic iridium and rhodium imine complexes, **7a** and **7b** respectively, with PhC≡CPh were investigated. The reactions were carried out at room temperature in CH₂Cl₂ and were monitored by ES-MS and in each case only one peak was observed, at *m/z* 668 and 578 respectively corresponding to replacement of MeCN by PhC≡CPh. The ¹H NMR spectra of the products, each show a 1 : 1 : 1 ratio of the Cp*, the imine ligand and PhC≡CPh, but no peaks due to coordinated NCMe are observed. In each complex, the Cp* is observed, 0.35 ppm upfield from the starting cationic complex, at *ca.* δ 1.38 suggesting a ring-current effect of an alkyne-insertion product. The other notable shift is that of the OMe signals which are observed at δ 2.48 and 2.35 for **7a** and **7b** respectively, more than 0.86 ppm upfield from the starting materials. These large shifts are in the opposite direction to that expected for coordination of the OMe to the metal centre and are again typical of ring-current effects. If after insertion of alkyne coordination of the OMe occurs it places the methyl in the vicinity of one of the Ph groups of the alkyne. Similar ring-current effects were seen on coordination of the OMe in Pd(PPh₃) complexes of this imine.²³ Hence the complexes are identified as **9a,b** containing a tridentate C,N,O ligand. For both **9a** and **9b**, the NCH₂ and CH₂O protons are observed as inequivalent multiplets, consistent with the chiral centre at the metal, and that epimerisation at the metal is slow on the NMR timescale.

The structure of **9a** has been determined by X-ray crystallography and is shown in Fig. 5 with selected bond lengths and angles. The structure confirms that the insertion of the alkyne into the Ir—C bond has resulted in the formation of a seven-membered ring and coordination of the OMe has formed a five-membered ring. The C(12)—Ir(1)—N(1) chelate bite angle [84.6(2)°] is larger than that for the N(1)—Ir(1)—O(1) angle [75.3(2)°], which is expected because of the larger chelate ring size.

Reaction of the phenyl-substituted imine **8a** with PhC≡CPh was tested since this does not have a pendant OMe group able to

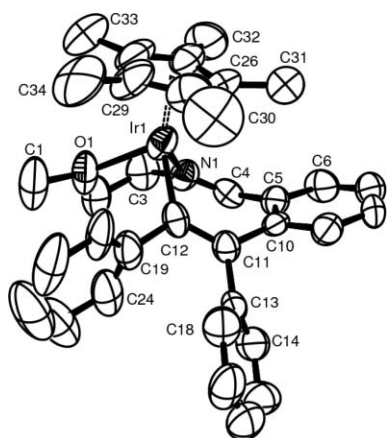


Fig. 5 Molecular structure and atom numbering scheme for the cation of **9a** with 50% displacement ellipsoids, all H atoms are omitted for clarity. Selected bond distances (Å) and angles (°): Ir(1)—C(12) 2.018(7), Ir(1)—N(1) 2.062(5), Ir(1)—O(1) 2.274(5), C(12)—Ir(1)—N(1) 84.6(2), C(12)—Ir(1)—O(1) 84.6(2), N(1)—Ir(1)—O(1) 75.3(2), C(12)—Ir(1)—O(1) 89.3(2).

stabilise the insertion product. The reaction was monitored by ES mass spectrometry, only an ion at m/z 358 was observed and there was no evidence for the expected insertion product. The reaction was worked up to give a light brown hexane soluble fraction and a deep brown insoluble fraction, unfortunately nothing could be isolated from the latter. The ^1H NMR spectrum of the hexane soluble fraction was rather uninformative showing a broad peak integrating to 1H at δ 3.90 and a sharp 1H singlet at δ 5.65 and multiplets integrating to 19H in the aromatic region. Fortunately, crystals suitable for X-ray diffraction were obtained and this allowed identification of the compound as amino indene **10**, the structure is shown in Fig. 6 with selected bond distances. The same compound, **10**, was also formed in the reaction of **6b** with $\text{PhC}\equiv\text{CPh}$, again unfortunately no metal-containing product was characterised.

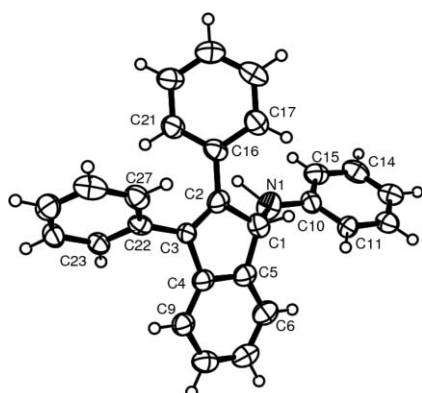
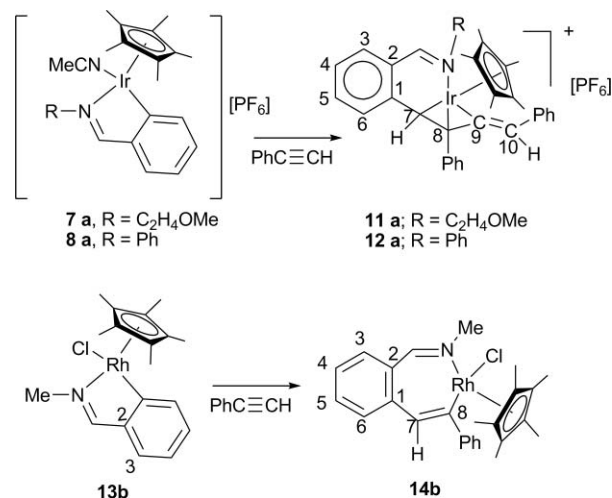


Fig. 6 Molecular structure and atom numbering scheme for **10** with 50% displacement ellipsoids. Selected bond distances (Å): C(1)—C(5) 1.503(5), C(1)—C(2) 1.513(5), C(2)—C(3) 1.354(5), C(3)—C(4) 1.486(5), C(4)—C(5) 1.394(5), N(1)—C(10) 1.371(4), N(1)—C(1) 1.428(4).

The structure shows an amino indene; the C(1)—N(1) bond length [1.428(4) Å] is typical of a single bond showing the imine

has been reduced to an amine. The product can be viewed as having been formed by insertion of $\text{PhC}\equiv\text{CPh}$ into the M—C bond of **8a** and then ring closure between the new metallated carbon and the imine carbon (*i.e.* C—C bond formation) and protonation at the nitrogen. Miura has reported catalytic formation of imino indenenes (formally dehydrogenation of **10**) using $[\text{Cp}^*\text{RhCl}_2]_2$ as a catalyst precursor.¹⁰ This is in contrast to reductive elimination by C—N bond formation as observed by Fagnou in formation of isoquinolines using the corresponding N^iBu imine complex of rhodium.¹⁴ Notably in that case the *t*-butyl substituent on the imine nitrogen is lost during the catalysis. Hence, it appears that the product of the reaction of $\text{PhC}\equiv\text{CPh}$ with cyclometallated imine complexes of Cp^*M (M = Ir, Rh) depends crucially on the substituent on the imine.¹⁰ The outcome of alkyne insertions into palladium cyclometallated imine complexes was similarly found to depend on the substituent on the imine, though no indenenes were found in those cases.²²

We have also investigated the reaction of iridium complexes **7a** and **8a** with $\text{PhC}\equiv\text{CH}$ (Scheme 3). The reaction of **7a** with $\text{PhC}\equiv\text{CH}$ in 1 : 1 ratio in CH_2Cl_2 was monitored by ES-MS. After 4 h two major ions were observed at m/z 592 and 490 assigned to a monoinsertion product and starting material respectively. After 7 h a further peak was observed at m/z 694 assigned to a diinsertion product. Thus the reaction appears to give a mixture of mono insertion and diinsertion with the second insertion occurring at a similar rate to the first one, as observed for the cyclometallated pyrazole complex **1a** discussed above. Therefore, the reaction was repeated using two equivalents of $\text{PhC}\equiv\text{CH}$. The ^1H NMR spectrum of the crude product showed only one species present with no signal for NCMe and the integration showing the incorporation of two equivalents of alkyne, this was confirmed by the FAB mass spectrum which showed an ion at m/z 694. The Cp^* resonance occurs at δ 1.69, similar to that, δ 1.75, in **7a**, suggesting that there is no ring-current effect in this case. Two singlets due to the alkyne protons are observed at δ 6.06 and 6.72, with the corresponding carbon signals at δ 48.45 and 121.18 respectively, and the NCH_2 protons give rise to two multiplets at δ 3.93 and 4.13; consistent with a chiral metal centre and slow epimerisation relative to the NMR timescale. The spectroscopic data is not able to unambiguously identify the product, fortunately,



Scheme 3

recrystallisation from dichloromethane–hexane gave X-ray quality crystals. The structure confirmed the formation of the diinsertion product **11a**. The crystal structure of this complex is shown in Fig. 7, with selected bond distances and angles.

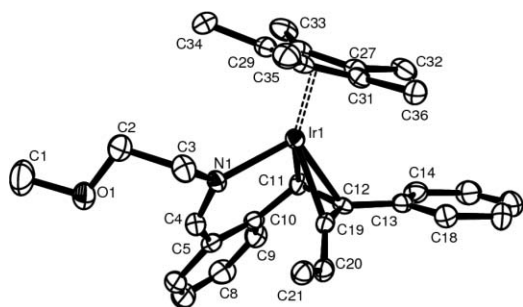


Fig. 7 Molecular structure and atom numbering scheme for the cation of **11a** with 50% displacement ellipsoids, only the ipso carbon C(21) of the terminal phenyl substituent is shown and all H atoms are omitted for clarity. Selected bond distances (Å) and angles (°): Ir(1)—C(19) 2.087(4), Ir(1)—N(1) 2.097(4), Ir(1)—C(11) 2.159(4), Ir(1)—C(12) 2.172(4), N(1)—C(4) 1.284(5), C(10)—C(11) 1.482(6), C(11)—C(12) 1.464(6), C(12)—C(19) 1.417(6), N(1)—Ir(1)—C(11) 90.20(16).

The structure shows the expected η^5 -Cp* and an eight-membered metallacycle formed by insertion of two molecules of PhC≡CH into the M—C bond of **7a**. The new ligand coordinates through the imine nitrogen and *via* three adjacent carbon atoms in a η^3 -allyl type interaction. This is analogous to the diinsertion product from a cyclometallated oxazoline.¹⁶ The bonding of the η^3 -allyl is slightly asymmetric with the Ir—C(19) bond length [2.087(4) Å] being shorter than the bonds to C(11) and C(12) [2.159(4) and 2.172(4) Å respectively]. The allyl is oriented with the central carbon atom (12) and its phenyl substituent C(13)—C(18) pointing up towards the Cp*, this is in contrast to the *anti* isomer we reported for the oxazoline analogue. The C(19)—C(20) distance, [1.326(6) Å], is typical of a double bond and is much shorter than the C(11)—C(12) bond length [1.464(6) Å] which is now part of the η^3 -allyl.

A similar reaction was attempted with the NPh-imine complex **6a**. The ¹H NMR spectrum of the crude product showed more than one Cp* signal, however after filtering the mixture through silica only one product was isolated. The ¹H NMR spectrum of the product shows a 1 : 1 : 2 ratio of the Cp*, imine and alkyne ligands as expected for the formation of a diinsertion product. The Cp* is observed at δ 1.51, similar to that, δ 1.47, in the starting chloride complex **6a**. Two singlets are observed at δ 5.20 and 6.72 assigned to (H⁷) and (H¹⁰) respectively. The FAB mass spectrum showed a molecular ion at m/z 712, confirming the presence of two molecules of PhC≡CH. The X-ray structure confirmed the product as **12a**, however, the data was not of sufficient quality to merit discussion of the bond lengths and angles.

As mentioned above, the products of the reactions of cyclometallated imines with PhC≡CPh seem to depend on the imine substituent. Hence, we decided to study further reactions of alkyl substituted imines. Jones has previously reported that the reactions of NMe substituted imine complexes **13a,b** with DMAD give the simple monoinsertion products.⁷ Fagnou, in a footnote, suggests that [RhCl₂Cp*]₂ catalysed synthesis of isoquinolines is much less

efficient starting from NMe imines than with the NtBu complex (8% *versus* 80% yield).¹⁴

The reaction of **13b** with PhC≡CPh in MeOH was attempted. After 5 min the ES-MS spectrum showed three signals at m/z 356 [**13b** – Cl], 397 [**13b** – Cl + MeCN] and 534 [**13b** – Cl + PhCCPh]. After 45 min a precipitate was formed, ES-MS and FAB mass spectra of the solid showed a peak at m/z 296, implying C–N bond reductive elimination to form an isoquinolinium salt and dissociation from the metal have taken place.²⁴ The ¹H NMR spectrum of the precipitate showed a mixture of products with two broad and intense signals in the Cp* region at δ 1.58 and 1.55 and one set of signals for the new cyclometallated ligand with an NMe signal at δ 3.36, however the Cp* and NMe signals are no longer in a 1 : 1 ratio. Unfortunately, we were unable to isolate any pure compounds by crystallisation or chromatography.

The corresponding reaction of **13b** with PhC≡CH was also examined. After 5 min the ES-MS spectrum showed three signals at m/z 356 [**13b** – Cl], 397 [**13b** – Cl + MeCN] and 458 [**13b** – Cl + PhCCH], a solid precipitated after 30 min and after 45 min only one peak was observed at m/z 458. The ¹H NMR spectrum of the solid showed one set of signals consistent with only one regioisomer of the expected monoinsertion product **14b**. The Cp* is observed at δ 1.35, 0.34 ppm upfield from **13b** as observed for the other alkyne insertion products discussed above. Fortunately the crystals which deposit from solution were suitable for X-ray diffraction and this confirmed the identity of the complex as **14b**. The structure of **14b** is shown in Fig. 8 with selected bond distances and angles.

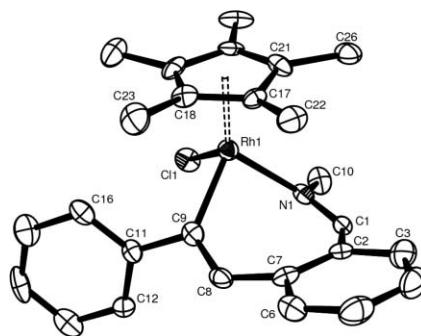


Fig. 8 Molecular structure and atom numbering scheme for **14b** with 50% displacement ellipsoids, all H atoms are omitted for clarity. Selected bond distances (Å) and angles (°): Rh(1)—C(9) 2.029(7), Rh(1)—N(1) 2.059(6), Rh(1)—C(1) 2.4130(19), C(8)—C(9) 1.365(9), C(9)—Rh(1)—N(1) 87.6(3), C(9)—Rh(1)—C(1) 90.0(2), N(1)—Rh(1)—C(1) 89.63(16).

Complex **14b** shows the expected 7-membered ring formed by insertion of the alkyne and that reductive elimination by C—N or C—C bond formation has not occurred yet. The structure confirms that the isomer formed has the phenyl group on the carbon attached to the metal with the hydrogen next to the original cyclometallated phenyl, the same as for **4b** discussed above. The M—C and M—N bond lengths [2.029(7) and 2.059(6) Å, respectively] are slightly shorter than the corresponding distances [2.061(7) and 2.096(6) Å, respectively] in the PhC≡CPh pyrazole insertion product **3b** described above, whilst the chelate angle C—M—N is larger [87.6(3) and 84.5(2)° in **14b** and **3b**, respectively].

However **14b** is not stable in solution, after a few hours in CDCl₃, a further reaction occurs and a new set of signals is

observed in the ^1H NMR spectrum. The Cp^* signal is observed at δ 1.63 a downfield shift of 0.30 ppm suggesting there is no longer a 7-membered chelate ring present, and the NMe signal is observed at δ 3.43. The FAB mass spectrum at this stage shows the same peak at m/z 458 (see above) and a new peak at m/z 220 consistent with reductive elimination of the C,N bond and formation of an isoquinolinium salt. Unfortunately, further purification by crystallisation or chromatography failed.

It appears that in contrast to Jones's results with DMAD,⁷ reaction of **13b** with $\text{PhC}\equiv\text{CPh}$ or $\text{PhC}\equiv\text{CH}$ gives insertion products that are unstable and spontaneously dissociate from the metal without the need for prior oxidation by copper(II) salts. However for the alkyl imines containing a functionalised side chain which is capable of coordinating, the products of insertion of $\text{PhC}\equiv\text{CPh}$ *i.e.* **9a,b** are stable. Pfeffer has previously commented on the extra stability of alkyne insertion products having very electron withdrawing substituents *e.g.* CO_2Me .¹⁵ These results are also consistent with Fagnou who showed that for N^iBu imine $\text{Cu}(\text{II})$ is not essential for isoquinoline formation.¹⁴ Notably, all of Fagnou's reactions involved dialkyl-substituted alkynes. We can also report that our attempts to follow Fagnou's reaction stoichiometrically have failed. Acetate-assisted cyclometallation of the N^iBu substituted imine with $[\text{RhCl}_2\text{Cp}^*]_2$ failed to give a clean cyclometallated product. We have noted in other cyclometallations, particularly with rhodium that the cyclometallation reactions can be equilibria, DFT calculations show that the process is close to thermoneutral for rhodium.²⁵

Miura has shown previously that the product of alkyne reactions with imines catalysed by Rh depends on the substituent on nitrogen and carbon of the imine.¹⁰ We have confirmed the importance of the substituent on nitrogen particularly in effecting the reductive elimination step. In addition, we have shown that the nature of the substituents on the alkyne also play a crucial role. The ease of cyclometallation and alkyne insertion suggests that facilitating the reductive elimination step is key to effective catalysis. In this regard the ability of a *t*Bu substituted cation to eliminate isobutene and a proton may play a crucial role in the catalysis reported by Fagnou.¹⁴ Interestingly, for the stoichiometric cyclometallation reaction to proceed in high yield is apparently not a requirement for catalysis.

Experimental

The reactions described were carried out under nitrogen using dry solvents; however, once isolated as pure solids the compounds can be handled in air. ^1H , and $^{13}\text{C}\{-^1\text{H}\}$ NMR spectra were obtained using Bruker 300, 400 or 500 MHz spectrometers, with CDCl_3 as solvent, unless otherwise stated. Chemical shifts were recorded in ppm (with tetramethylsilane as internal reference). FAB mass spectra were obtained on a Kratos concept mass spectrometer using NOBA as matrix. The electrospray (ES) mass spectra were recorded using a micromass Quattro LC mass spectrometer with dichloromethane or methanol as solvent. Infrared spectra were run as solids in a diamond ATR cell using a Perkin Elmer Spectrum 1 instrument. Microanalyses were performed by the Elemental Analysis Service (University of North London). All starting materials were obtained from Aldrich, with the exception of $[\text{MCl}_2\text{Cp}^*]_2$ ($\text{M} = \text{Rh}, \text{Ir}$)²⁶ and $[\text{RuCl}_2(p\text{-cymene})]_2$,²⁷ complexes

1a-c,¹⁷ **5a,b** **6a,b**² and **13a,b**⁷ which were prepared by literature methods.

Preparation of (2a)

A mixture of $[\text{IrCl}(\text{phenylpyrazole})\text{Cp}^*]$ **1a** (50 mg, 0.099 mmol) and DMAD (17 mg, 0.12 mmol) in MeOH (5 mL) was stirred for 1 h at RT. The solution was rotary evaporated to dryness. The solid was washed with hexane and recrystallised from CH_2Cl_2 –hexane to give **2a** (30.0 mg, 51%) as yellow crystals. Anal. Calcd for $\text{C}_{25}\text{H}_{28}\text{ClIrN}_2\text{O}_4$: C, 46.33, H, 4.35, N, 4.32. Found: C, 46.33, H, 4.41, N, 4.25%. ^1H NMR: δ 1.31 (s, 15H, Cp^*), 3.64 (s, 3H, OMe), 3.69 (s, 3H, OMe), 6.51 (t, 1H, J 2.5, H^2), 7.17 (dd, 1H, J 8.0, 1.0, H^5), 7.34 (td, 1H, J 8.0, 2.0, H^6), 7.43 (m, 2H, H^7 , H^8), 7.81 (dd, 1H, J 2.5, 0.5, H^3), 8.21 (dd, 1H, J 2.5, 0.5, H^1). ^{13}C NMR: δ 8.33 (C_5Me_5), 50.14 (OMe), 51.80 (OMe), 89.34 (C_5Me_5), 108.84 (C^2), 127.29 (C^5), 127.49, 128.68 ($\text{C}^{7,8}$), 133.21 (C^6), 134.37 (C^3), 132.30, 136.88, 138.45 ($\text{C}^{4,9,10}$), 145.48 (C^1), 167.64, 168.08 ($2 \times \text{CO}_2\text{Me}$), 176.15 (C^{11}). ES-MS m/z 613 $[\text{M}-\text{Cl}]^+$, MS FAB m/z 613 $[\text{M}-\text{Cl}]^+$, 648 $[\text{M}]^+$.

Preparation of 2b

A mixture of **1b** (50 mg, 0.12 mmol) and DMAD (14 mg, 0.12 mmol) in MeOH (5 ml) was stirred for 5 h at RT. The solution was rotary evaporated to dryness. The product was washed with hexane and recrystallised from CH_2Cl_2 /hexane to give **2b** (55.0 mg, 81%) as yellow crystals. Anal. Calcd for $\text{RhC}_{25}\text{H}_{28}\text{N}_2\text{O}_4\text{Cl}$: C, 53.73, H 5.05, N, 5.01. Found: C 53.53, H 5.17, N 4.92%. ^1H NMR: δ 1.30 (s, 15H, Cp^*), 3.64 (s, 3H, OMe^{13}), 3.67 (s, 3H, OMe^{15}), 6.50 (t, 1H, J 2.5, H^2), 7.20 (dd, 1H, J 8.0, 1.0, H^5), 7.36 (ddd, 1H, J 8.0, 6.0, 2.0, H^6), 7.46 (m, 2H, H^7 , H^8), 7.82 (dd, 1H, J 2.5, 0.5, H^3), 8.27 (dd, 1H, J 2.5, 0.5, H^1). ^{13}C NMR (500 Mhz): 8.57 (C_5Me_5), 50.35 (OMe^{13}), 51.88 (OMe^{15}), 96.89 (d, J_{RhC} 25, C_5Me_5), 108.94 (C^2), 127.44 (C^5), 127.68 (C^6), 128.61, 133.20 ($\text{C}^{7,8}$), 134.53 (C^3), 130.94, 136.99, 137.10 ($\text{C}^{4,9,10}$), 146.26 (C^1), 166.37, 174.39 ($2 \times \text{CO}_2\text{Me}$), 181.60 (d, J_{RhC} 135, C^{11}). ES-MS m/z ($\text{M}-\text{Cl}$) 523, MS (FAB) m/z 523 $[\text{M}-\text{Cl}]^+$.

Preparation of 2c

A mixture of **1c** (39 mg, 0.09 mmol), DMAD (16 mg, 0.13 mmol) in MeOH (5 ml) was stirred for 3 h at room temperature, under N_2 . The solution was rotary evaporated to dryness, washed with hexane and recrystallised from CH_2Cl_2 –hexane to give **2c** (41 mg, 78%) as brown crystals. Anal. Calcd for $\text{C}_{25}\text{H}_{27}\text{ClN}_2\text{O}_4\text{Ru}\cdot\text{CH}_2\text{Cl}_2$: C, 48.72, H, 4.56, N, 4.37. Found: C, 49.89, H, 3.53, N, 4.13%. ^1H NMR: δ 1.06 (d, J 7.0, 3H, CHMeMe'), 1.16 (d, J 7.0, 3H, CHMeMe'), 2.11 (s, 3H, $\text{Me}(\text{Cy})$), 2.64 (sept, J 7.0, 1H CHMeMe'), 3.63 (s, 3H, OMe), 3.64 (s, 3H, OMe), 4.12 (d, 1H, J 5.5, Cy), 4.44 (d, 1H, J 5.5, Cy), 4.54 (d, 1H, J 5.5, Cy), 5.52 (d, 1H, J 5.5, Cy), 6.47 (t, 1H, J 2.0, H^2), 7.19 (d, 1H, J 8.0, H^5), 7.41 (td, 1H, J 8.0, 1.5, H^6), 7.51 (m, 2H, H^7 , H^8), 7.78 (d, 1H, J 1.5, H^3), 8.38 (d, 1H, J 1.5, H^1), ^{13}C NMR: δ 18.80 ($\text{Me}(\text{Cy})$), 22.64 ($\text{MeMe}'\text{CH}$), 22.97 ($\text{MeMe}'\text{CH}$), 30.94 ($\text{MeMe}'\text{CH}$), 50.10, 51.78 ($2 \times \text{OMe}$), 80.71, 82.40, 83.07, 92.81 ($4 \times \text{CH}$, Cy), 102.84 (Cq , Cy), 108.35 (C^3), 109.37 (Cq , Cy), 126.38 (C^5), 127.45 (C^6), 128.54, 132.90 ($\text{C}^{7,8}$), 134.22 (C^2), 130.66, 137.41, 139.68 ($\text{C}^{4,9,10}$), 145.25 (C^1), 164.69, 175.47 ($2 \times \text{CO}_2\text{Me}$), 190.94 (C^{11}). ES-MS m/z 521 $[\text{M}-\text{Cl}]^+$, FAB MS m/z 556 $[\text{M}]^+$, 521 $[\text{M}-\text{Cl}]^+$.

Preparation of 3a

A mixture of **1a** (50 mg, 0.10 mmol) and PhC≡CPh (19 mg, 0.11 mmol) in MeOH (5 ml) was stirred for 3 h at RT. The solution was rotary evaporated to dryness. The product was washed with hexane and recrystallised from CH₂Cl₂–hexane to give **3a** (42 mg, 62%) as yellow crystals. Anal. Calcd for C₃₃H₃₂ClIrN₂·CHCl₃: C, 50.81, H, 4.14, N, 3.49. Found: C, 50.81, H, 4.28, N, 3.40%. ¹H NMR: δ 1.36 (s, 15H, Cp*), 6.56 (t, 1H, *J* 2.5, H²), 6.67 (t, 1H, *J* 7.0, Ph), 6.71 (dd, 2H, *J* 8.0, 1.5, Ph), 6.83 (tt, 1H, *J* 7.5, 1.5, Ph), 6.91 (td, 2H, *J* 7.0, 1.0, Ph), 7.18 (m, 1H, Ph), 7.20 (t, 1H, *J* 2.0, Ph), 7.22 (d, 1H, *J* 1.0, Ph), 7.24 (dd, 1H, *J* 5.0, 5.5, Ph), 7.26 (t, 1H, *J* 2.5, Ph), 7.34 (m, 2H, Ph), 7.52 (m, 1H, Ph), 7.91 (dd, *J* 2.5, 1.0, 1H, H³), 8.41 (dd, *J* 2.5, 1.0, 1H, H¹). ¹³C NMR: δ 8.79 (C₅Me₅), 88.46 (C¹⁸), 108.36 (C²), 122.79, 124.34, 125.43, 126.51, 126.64, 131.60, 131.80 (CH, Ph), 133.77 (C³), 134.45 (CH, Ph), 136.82, 138.54 (Ar Cq or C¹⁰), 144.62 (C¹), 145.19, 147.65, 154.22, (Ar Cq or C¹⁰), 161.23 (C¹¹). ES-MS *m/z* 647 [M-Cl]⁺, MS FAB *m/z* 647 [M-Cl]⁺, 684 [M]⁺

Preparation of 3b

A mixture of **1b** (70 mg, 0.17 mmol) and PhC≡CPh (33 mg, 0.18 mmol) in MeOH (7 ml) was stirred at room temperature for 3 h. The solution was rotary evaporated to dryness and the solid was dissolved in CH₂Cl₂ and filtered through Celite. The filtrate was evaporated to dryness and the solid was washed with hexane to give **3b** (80 mg, 81%) as an orange solid. Anal. Calcd for C₃₃H₃₂ClN₂Rh: C 66.62, H 5.42, N 4.71. Found: C 66.53, H 5.41, N 4.79%. ¹H NMR: δ 1.35 (s, 15H, Cp*), 6.56 (t, 1H, *J* 2.5, H²), 6.72 (m, 4H, Ph), 6.85 (m, 2H, Ph), 6.92 (m, 3H, Ph), 7.25 (m, 5H, Ph), 7.92 (dd, 1H, *J* 3, 0.5, H³), 8.56 (dd, 1H, *J* 2, 1, H¹). ¹³C NMR: δ 9.07 (C₅Me₅), 96.09 (d, *J*_{RhC} 6.5, C₅Me₅), 108.40 (C²), 123.10, 124.55, 125.92, 126.57, 127.01, 128.40, 131.13 (CH, Ph), 133.77 (C³), 134.54 (CH, Ph), 136.89, 137.04, 143.25 (Ar Cq or C¹⁰), 145.78 (C¹), 146.71, 152.66 (ArCq or C¹⁰), 176.08 (d, *J*_{RhC} 30.5, C¹¹). ES-MS: *m/z* 559 [M-Cl]⁺. MS FAB: *m/z* 594 [M]⁺, 559 [M-Cl]⁺.

Preparation of 3c

A mixture of **1c** (50 mg, 0.12 mmol) and PhC≡CPh (23 mg, 0.13 mmol) in MeOH (5 ml) was stirred for 1 h at RT. The solution was rotary evaporated to dryness. The product was washed with hexane and recrystallised from CH₂Cl₂–hexane to give **3c** (30 mg, 42%) as brown crystals. Anal. Calcd for C₃₃H₃₁ClN₂Ru: C, 66.94, H, 5.28, N, 4.73. Found: C, 66.95, H, 5.34, N, 4.65%. ¹H NMR: δ 1.08 (d, *J* 7.0, 3H, CHMeMe'), 1.23 (d, *J* 7.0, 3H, CHMeMe'), 2.44 (s, 3H, Me, Cy), 2.79 (sept, 1H, *J* 7.0, CHMeMe'), 3.48 (dd, 1H, *J* 6.0, 1.0, Cy), 4.49 (dd, 1H, *J* 6.0, 1.0, Cy), 4.63 (dd, 1H, *J* 6.0, 1.0, Cy), 5.54 (dd, 1H, *J* 6.0, 1.0, Cy), 6.50 (t, 1H, *J* 2.5, H²), 6.75 (m, 4H, Ph), 6.86 (tt, 1H, *J* 7.0, 1.5, Ph), 6.93 (tm, 3H, *J* 7.0, Ph), 7.22 (dt, 1H, *J* 7.0, 1.0, H⁸), 7.26 (m, 1H, H^{6,7}), 7.29 (m, 1H, H^{6,7}), 7.30 (m, 2H, Ph), 7.34 (m, 1H, H⁵), 7.85 (dd, 1H, *J* 2.5, 1.0, H³), 8.57 (dd, 1H, *J* 2.5, 1, H¹). ¹³C NMR δ 19.48 (Me, Cy), 23.04 (MeMe'CH), 23.46 (MeMe'CH), 31.21 (MeMe'CH), 75.14, 78.71, 80.91, 96.25 (4 × CH, Cy), 103.65 (Cq, Cy), 107.69 (C²), 110.22 (Cq, Cy), 122.99, 124.53, 125.36, 125.76, 126.19, 127.04, 128.00, 128.34, 131.41 (CH, Ph), 133.24 (C³), 133.55 (C⁵), 137.40, 137.57 (Cq, Ar or C¹⁰), 143.98 (C¹), 145.90, 146.62, 152.32 (Cq, Ar

or C¹⁰), 183.19 (C¹¹). ES-MS (ESI) *m/z* 557 [M-Cl]⁺, MS (FAB) *m/z* 557 [M-Cl]⁺

Preparation of 4b

A mixture of **1b** (66 mg, 0.16 mmol) and PhC≡CH (18 mg, 0.17 mmol) in MeOH (7 ml) was stirred at room temperature for 2 h. The solution was rotary evaporated to dryness. The solid was dissolved in CH₂Cl₂ and filtered through Celite. The filtrate was evaporated to dryness and the crude product was purified by passing through a short silica column, using CH₂Cl₂ as the first eluent and MeOH–CH₂Cl₂ (1 : 9) as the second eluent. The second fraction was rotary evaporated to dryness to give **4b** (30 mg, 36%) as an orange solid. Anal. Calcd for C₂₇H₂₈ClN₂Rh: C 62.50, H 5.44, N 5.40. Found: C 62.58, H 5.34, N 5.36%. ¹H NMR: δ 1.30 (s, 15H, Cp*), 6.48 (t, 1H, *J* 2.5, H²), 7.05 (m, 1H, H¹⁵), 7.07 (s, 1H, H¹⁰), 7.15 (m, 4H, H¹³ H¹⁴), 7.24 (m, 2H, H⁵, H⁶), 7.39 (ddd, 1H, *J* 8.0, 6.0, 2.0, H⁷) 7.46 (dt, 1H, *J* 8.0, 1.0, H⁸), 7.76 (dd, 1H, *J* 2.5, 1.0, H³), 8.46 (dd, 1H, *J* 2.5, 1.0, H¹). ¹³C NMR: 9.21 (C₅Me₅), 95.82 (d, *J*_{RhC} 25, C₅Me₅), 108.41 (C²), 124.77 (C¹⁵), 125.57, 126.17 (C^{5,6}), 126.68, 126.88 (C^{13,14}), 128.10 (C⁷), 128.35 (C¹⁰), 132.81 (C⁸), 134.26 (C³), 135.27, 138.38, 152.85 (Cq, C⁴ C⁹ C¹²), 145.48 (C¹), 178.64 (d, *J*_{RhC} 125, C¹¹). ES-MS *m/z* 483 [M-Cl]⁺

Preparation of 7a

KPF₆ (48 mg, 0.26 mmol) was added to a solution of **5a** (70 mg, 0.13 mmol), in acetonitrile (10 ml). The mixture was stirred overnight, then filtered through Celite to remove excess KPF₆. The filtrate was evaporated to dryness and washed with hexane to give **7a** as a brown solid (70 mg, 78%) which could be recrystallised from dichloromethane–hexane. Anal. Calcd for C₂₂H₃₀F₆N₂OIrP: C, 39.11, H, 4.48, N, 4.15. Found: C, 38.95, H, 4.69, N, 3.97%. ¹H NMR: δ 1.75 (s, 15H, Cp*), 2.36 (s, 3H, NCMe), 3.34 (s, 3H, OMe), 3.66 (m, 1H, CHHO), 3.84 (dt, 1H, *J* 10, 2.5, CHHO), 4.17 (m, 2H, NCH₂), 7.11 (t, 1H, *J* 7.5, H⁴), 7.22 (dt, 1H, *J* 7.5, 1, H⁵), 7.60 (d, 1H, *J* 7.5, H³), 7.69 (d, 1H, *J* 7, H⁶), 8.40 (s, 1H, HC=N). ¹³C NMR: δ 3.71 (NCMe), 9.10 (C₅Me₅), 58.88 (OMe), 61.65 (CH₂O), 69.50 (NCH₂), 91.52 (C₅Me₅), 119.16 (NCMe), 123.87, 129.52, 132.69, 134.65 (C³, C⁴, C⁵, C⁶), 146.92 (C²), 162.29 (C¹Ir), 179.28 (HC=N). MS (FAB): *m/z* 490 [M-NCMe]⁺. IR: ν(C=N) 1606 cm⁻¹.

Preparation of 7b

KPF₆ (113 mg, 0.61 mmol) was added to a solution of **5b** (134 mg, 0.31 mmol), in acetonitrile (10 ml). The mixture was stirred overnight, then filtered through Celite to remove excess KPF₆. The filtrate was evaporated to dryness and washed with hexane to give **7b** as a yellow solid (181 mg, 86%). Anal. Calcd for C₂₂H₃₀F₆N₂OPRh: C, 45.06, H, 5.16, N, 4.78. Found: C, 45.14, H, 5.21, N, 4.55%. ¹H NMR: δ 1.70 (s, 15H, Cp*), 2.23 (s, 3H, NCMe), 3.36 (s, 3H, OMe), 3.74 (m, 1H, CHHO), 3.90 (dt, 1H, *J* 10, 3, CHHO), 4.01 (m, 1H, NCHH'), 4.16 (m, 1H, NCHH'), 7.16 (dt, 1H, *J* 7.5, 1, H⁴), 7.31 (dt, 1H, *J* 7.5, 1.5, H⁵), 7.52 (dd, 1H, *J* 7.5, 1.5, H³), 7.72 (d, 1H, *J* 7.5, H⁶), 8.24 (d, 1H, *J*_{RhH} 4, HC=N). ¹³C NMR: δ 3.54 (NCMe), 9.42 (C₅Me₅), 58.91 (OMe), 60.43 (CH₂O), 69.85 (NCH₂), 98.29 (d, *J*_{RhC} 7, C₅Me₅), 124.44, 129.43, 131.96, 135.51 (C³, C⁴, C⁵, C⁶), 145.96 (C²), 176.37

(HC=N), C¹Rh (not observed). MS (FAB): *m/z* 400 [M-NCMe]⁺. IR: $\nu(\text{C}=\text{N})$ 1614 cm⁻¹.

Preparation of 8a

A mixture of **6a** (130 mg, 0.24 mmol), KPF₆ (130 mg, 0.71 mmol) in acetonitrile (10 ml); was stirred for 24 h, then filtered through Celite to remove excess KPF₆. The filtrate was evaporated to dryness and washed with hexane to give to give **8a** (120 mg, 72%) as an orange precipitate. Anal. Calcd for C₂₅H₂₈F₆IrN₂P·CH₂Cl₂: C, 40.10, H, 3.85, N, 3.60. Found: C, 39.57, H, 3.10, N, 3.03%. ¹H NMR: δ 1.51 (s, 15H, Cp*), 2.49 (s, 3H, NCMe), 7.19 (dt, 1H, *J* 7.5, 1, H⁴), 7.30 (dt, 1H, *J* 7.5, 1.5, H⁵), 7.40 (m, 3H, Ph), 7.56 (m, 2H, Ph), 7.73 (dd, 1H, *J* 7.5, 1, H³), 7.80 (d, 1H, *J* 7.5, H⁶), 8.42 (s, 1H, HC=N). ¹³C NMR: δ 3.72 (NCMe), 8.61 (C₅Me₅), 91.93 (C₅Me₅), 120.06 (NCMe), 122.31, 124.07, 128.58, 130.11, 130.82, 133.61, 135.00 (C³, C⁴, C⁵, C⁶ and Ph), 147.42 (C²), 149.83 (Ph), 163.67 (C¹Ir), 178.13 (HC=N). MS (FAB): *m/z* 549 [M]⁺, 508 [M-NCMe]⁺. IR: $\nu(\text{C}=\text{N})$ 1583 cm⁻¹.

Preparation of 9a

PhC≡CPh (11 mg, 0.06 mmol) was added to solution of **7a** (40 mg, 0.06 mmol) in dichloromethane (5 ml); after stirring for 30 h, the solution was evaporated to dryness and then washed with hexane to give **9a** as a yellow precipitate (40 mg, 83%). Anal. Calcd for C₃₄H₃₇F₆IrNOP: C, 50.24, H, 4.59, N, 1.72. Found: C, 50.00, H, 4.47, N, 1.64%. ¹H NMR: δ 1.39 (s, 15H, Cp*), 2.48 (s, 3H, OMe), 3.21 (m, 1H, CHH'O), 3.32 (m, 1H, CHH'O), 4.13 (m, 2H, NCH₂), 6.72 (m, 2H, Ph), 6.97 (m, 6H, H⁴, H⁵, Ph), 7.29 (m, 5H, H⁶, Ph), 7.59 (m, 1H, H³), 9.14 (s, 1H, HC=N). ¹³C NMR: δ 9.04 (C₅Me₅), 61.53 (OMe), 65.51 (CH₂O), 73.14 (NCH₂), 89.18 (C⁹), 99.07 (C₅Me₅), 125.45, 126.37, 127.52, 128.63, 131.37, 131.94, 132.26, 132.10, 134.13 (Ar-H), 141.86, 144.65, 145.65, 149.49, 158.93 (Ph Cq and C^{7,8}), 170.84 (HC=N). MS (FAB): *m/z* 668 [M]⁺. IR: $\nu(\text{C}=\text{N})$ 1595 cm⁻¹.

Preparation of 9b

PhC≡CPh (5.2 mg, 0.03 mmol) was added to solution of **5b** (16 mg, 0.03 mmol) in CDCl₃ in an NMR tube, after 30 h, the solution was evaporated to dryness and then washed with hexane to give **7b** as a yellow precipitate (18 mg, 85%). ¹H NMR: δ 1.36 (s, 15H, Cp*), 2.35 (s, 3H, OMe), 3.04 (m, 1H, CHH'O), 3.43 (m, 1H, CHH'O), 4.05 (m, 1H, NCHH'), 4.23 (m, 1H, NCHH'), 6.75 (m, 2H, Ph), 6.95 (m, 4H, H⁴, H⁵, Ph), 7.08 (m, 1H, Ph), 7.33 (m, 5H, H⁶, Ph), 7.53 (m, 1H, Ph), 7.64 (m, 1H, H³), 9.14 (d, 1H, *J* 3, HC=N). MS (FAB): *m/z* 578 [M]⁺. IR: $\nu(\text{C}=\text{N})$ 1596 cm⁻¹.

Preparation of 10

From **8a**: PhC≡CPh (51.4 mg, 0.29 mmol) was added to solution of **8a** (100 mg, 0.14 mmol) in dichloromethane and refluxed for 20 h. After this time the solution was evaporated to dryness washed with hexane to give a light brown hexane soluble and a deep brown insoluble fraction. The latter was washed through silica, however, no pure fraction could be isolated. Compound **10** was isolated from the hexane soluble fraction as an orange solid (23 mg, 45%). From **6b**: PhC≡CPh (23.7 mg, 0.13 mmol) was added to solution of **6b** (60 mg, 0.13 mmol) in dichloromethane was stirred for 8 h

and then the solvent exchanged by NCMe and refluxed for 18 h. The solution was evaporated to dryness and washed with hexane to give a light brown hexane soluble from which **10** was isolated as an orange solid (24 mg, 50%). Anal. Calcd for C₂₇H₂₁N: C, 90.21, H, 5.89, N, 3.90. Found: C, 90.03, H, 5.81, N, 3.80%. ¹H NMR: δ 3.90 (br, 1H NH), 5.65 (s, 1H, CH), 6.45 (d, 1H, *J* 7, Ph), 6.69 (m, 3H, Ph) 6.90 (m, 1H, Ph) 6.93 (d, 2H, *J* 7, Ph), 7.1–7.6 (m, 12H, Ph). MS (FAB): *m/z* 358 [M]⁺.

Preparation of 11a

PhC≡CH (30 mg, 0.30 mmol) was added to solution of **7a** (100 mg, 0.15 mmol) in dichloromethane; after stirring for 30 h, **11a** was isolated as a yellow precipitate (105 mg, 85%). Anal. Calcd for C₃₆H₃₉F₆IrNOP: C, 51.54, H, 4.69, N, 1.67. Found: C, 51.22, H, 4.59, N, 1.59%. ¹H NMR: δ 1.69 (s, 15H, Cp*), 3.06 (m, 2H, CH₂O), 3.14 (s, 3H, OMe), 3.93 (m, 1H, NCHH'), 4.13 (m, 1H, NCHH'), 6.06 (s, 1H, H⁷), 6.72 (s, 1H, H¹⁰), 7.46 (m, 8H, H⁴, H⁵, (2 × Ph, H_m, H_p)), 7.73 (m, 5H, H³, (2 × Ph, H_o)), 8.04 (d, 1H, *J* 8, H⁶), 8.09 (s, 1H, HC=N). ¹³C NMR: δ 9.05 (C₅Me₅), 48.95 (C⁷), 53.65 (C_q), 58.65 (OMe), 70.72 (CH₂O), 71.73 (NCH₂), 80.18 (C_q), 99.07 (C₅Me₅), 121.18 (C¹⁰), 127.57, 127.81, 129.00, 129.30, 130.06, 130.23, 131.17, 135.53, 136.34 (CH, Ph), 128.09, 129.20, 133.39, 135.18, 150.17 (all C_q), 167.90 (HC=N). MS (FAB): *m/z* 694 [M]⁺. IR: $\nu(\text{C}=\text{N})$ 1615 cm⁻¹.

Preparation of 12a

PhC≡CH (34 mg, 0.33 mmol) and KPF₆ (76 mg, 0.41 mmol) were added to solution of **6a** (90 mg, 0.17 mmol) in NCMe; after stirring for 7 h, NCMe was replaced by dichloromethane and the solution stirred for a further 21 h. After this time the solvent was evaporated and the solid was washed through a small plug of silica (CH₂Cl₂/NCMe). The solvent was evaporated to give **12a** as a red precipitate (92 mg, 65%). Anal. Calcd for C₃₆H₃₇F₆IrNP: C, 54.66, H, 4.35, N, 1.63. Found: C, 54.51, H, 4.23, N, 1.53%. ¹H NMR (in d₄-MeOH): δ 1.51 (s, 15H, Cp*), 5.20 (s, 1H, H⁷), 6.72 (s, 1H, H¹⁰), 6.89 (m, 2H, 2 × Ph), 7.01 (m, 3H, H⁴, 2 × Ph), 7.20 (m, 4H, H⁶, 2 × Ph), 7.54 (m, 8H, Ph), 7.92 (dt, 1H, *J* 7.5, 1.5, H⁵), 8.02 (d, 1H, *J* 7.5, H³), 8.18 (s, 1H, HC=N). MS (FAB): *m/z* 712 [M]⁺. IR: $\nu(\text{C}=\text{N})$ 1615 cm⁻¹.

Preparation of 14b

PhC≡CH (10 mg, 0.09 mmol) was added to a solution of complex **13b** (50 mg, 0.13 mmol) in MeOH (5 mL). The reaction was monitored by ESI, and after 5 min showed mostly *m/z* 458 (mono insertion), and traces of **13b**. Over a period of 30 min an orange precipitate formed which was collected by filtration (12 mg, 19%). ¹H NMR: δ 1.35 (s, 15H, Cp*), 3.89 (s, 3H, Me), 7.11 (m, 2H, Ph), 7.22 (m, 6H, Ph), 7.32 (d, 1H, *J* 7.5, H⁶), 7.40 (dd, 1H, *J* 6.0, 7.0, H³), 8.63 (s, 1H, NCH)

X-ray crystal structure determinations

Details of the structure determinations of crystals of **2a–c**, **3a**, **7b**, **8a**, **9a**, **10**, **11a**, and **14b** are given in Tables 1 and 2 (Complexes **3b,c** are included in the supplementary material[†]). Data were collected on a Bruker Apex 2000 CCD diffractometer using graphite monochromated Mo-K α radiation, $\lambda = 0.7107 \text{ \AA}$ at

Table 1 Crystallographic data for **2a–c, 3a and 7b**

	2a	2b	2c	3a	7b
Empirical formula	C ₂₅ H ₂₈ ClIrN ₂ O ₄	C ₂₅ H ₂₈ ClN ₂ O ₄ Rh	C ₂₆ H ₂₉ Cl ₃ N ₂ O ₄ Ru	C ₃₄ H ₃₃ Cl ₄ IrN ₂	C ₂₂ H ₃₀ F ₆ N ₂ OPRh
Formula weight	648.14	558.85	640.93	803.62	586.36
Temperature	150(2) K	150(2) K	150(2) K	150(2) K	150(2) K
Crystal system	Monoclinic	Monoclinic	Triclinic	Monoclinic	Orthorhombic
Space group	<i>P</i> 2 ₁ / <i>n</i>	<i>P</i> 2 ₁ / <i>n</i>	<i>P</i> $\bar{1}$	<i>P</i> 2 ₁ / <i>n</i>	<i>Pbca</i>
<i>a</i> /Å	10.0222(18)	10.0361(17)	9.240(6)	12.990(2)	11.7650(5)
<i>b</i> /Å	16.342(3)	16.349(3)	9.619(6)	15.877(3)	17.6433(7)
<i>c</i> /Å	15.312(3)	15.289(3)	16.215(11)	15.564(3)	24.0030(9)
α /°	90		91.764(11)		90
β /°	106.030(3)	106.251(3)	103.811(11)	99.493(3)	90
γ /°	90		108.957(11)		90
<i>U</i> /Å ³	2410.4(8)	2408.4(7)	1314.4(15)	3166.0(9)	4982.4(3)
<i>Z</i>	4	4	2	4	8
Density (calc.) Mg m ⁻³	1.786	1.541	1.619	1.686	1.563
μ /mm ⁻¹	5.684	0.854	0.937	4.582	0.811
<i>F</i> (000)	1272	1144	652	1584	2384
Crystal size mm	0.11 × 0.10 × 0.07	0.22 × 0.19 × 0.07	0.24 × 0.17 × 0.05	0.25 × 0.16 × 0.05	0.25 × 0.23 × 0.17
Theta range	1.86 to 26.99	1.86 to 26.99	2.25 to 26.00	1.85 to 26.00	1.70 to 25.00
Index ranges	-12 ≤ <i>h</i> ≤ 12, -20 ≤ <i>k</i> ≤ 20, -19 ≤ <i>l</i> ≤ 19	-12 ≤ <i>h</i> ≤ 12, -20 ≤ <i>k</i> ≤ 20, -19 ≤ <i>l</i> ≤ 19	-11 ≤ <i>h</i> ≤ 11, -11 ≤ <i>k</i> ≤ 11, -19 ≤ <i>l</i> ≤ 19	-15 ≤ <i>h</i> ≤ 16, -19 ≤ <i>k</i> ≤ 19, -18 ≤ <i>l</i> ≤ 19	-13 ≤ <i>h</i> ≤ 13, -20 ≤ <i>k</i> ≤ 20, -28 ≤ <i>l</i> ≤ 28
Reflections collected	19930	19939	10350	24390	34225
Independent reflections (<i>R</i> _{int})	5258 [<i>R</i> _{int} = 0.0758]	5252 [<i>R</i> _{int} = 0.0606]	5086 [<i>R</i> _{int} = 0.0757]	6211 [<i>R</i> _{int} = 0.0956]	4377 [<i>R</i> _{int} = 0.0331]
Data/restraints/parameters	5258/0/304	5252/0/305	5086/0/330	6211/0/375	4377/0/305
Goodness-of-fit, <i>F</i> ²	0.916	0.974	0.992	0.899	1.073
Final <i>R</i> indices [<i>I</i> > 2σ(<i>I</i>)]	<i>R</i> ₁ = 0.0358, <i>wR</i> ₂ = 0.0591	<i>R</i> ₁ = 0.0357, <i>wR</i> ₂ = 0.0715	<i>R</i> ₁ = 0.0561, <i>wR</i> ₂ = 0.1283	<i>R</i> ₁ = 0.0419, <i>wR</i> ₂ = 0.0714	<i>R</i> ₁ = 0.0353, <i>wR</i> ₂ = 0.0882
<i>R</i> indices (all data)	<i>R</i> ₁ = 0.0488, <i>wR</i> ₂ = 0.0625	<i>R</i> ₁ = 0.0473, <i>wR</i> ₂ = 0.0750	<i>R</i> ₁ = 0.0686, <i>wR</i> ₂ = 0.1340	<i>R</i> ₁ = 0.0648, <i>wR</i> ₂ = 0.0770	<i>R</i> ₁ = 0.0392, <i>wR</i> ₂ = 0.0903
Largest diff. peak and hole/e Å ⁻³	1.620 and -1.507	0.627 and -0.561	1.262 and -1.09	1.447 and -1.283	1.041 and -0.715

Table 2 Crystallographic data for **8a, 9a, 10, 11a, 14b**

	8a	9a	10	11a	14b
Empirical formula	C ₂₅ H ₂₈ F ₆ IrN ₂ P	C ₃₄ H ₃₈ ClF ₆ IrNOP	C ₂₇ H ₂₁ N	C ₃₇ H ₄₀ Cl ₂ F ₆ IrNOP	C ₂₆ H ₂₆ ClNRh
Formula weight	693.66	855.28	359.45	922.77	493.86
Temperature	150(2) K	290(2) K	150(2) K	150(2) K	150(2) K
Crystal system	Orthorhombic	Tetragonal	Monoclinic	Monoclinic	Orthorhombic
Space group	<i>P</i> 2 ₁ / <i>n</i>	<i>P</i> -42(1) <i>c</i>	<i>P</i> 2 ₁ / <i>c</i>	<i>P</i> 2 ₁ / <i>c</i>	<i>Pbca</i>
<i>a</i> /Å	8.6691(4)	21.2244(8)	10.669(5)	11.807(6)	13.159(4)
<i>b</i> /Å	27.6056(12)	21.2244(8)	8.067(4)	14.582(8)	14.219(4)
<i>c</i> /Å	11.2039(5)	15.9689(8)	22.852(11)	21.324(12)	23.675(7)
α /°	90		90	90	90
β /°	110.8060(10)	90	102.836(9)	95.270(9)	90
γ /°	90	90	90	90	90
<i>U</i> /Å ³	2506.42(19)	7193.6(5)	1917.6(16)	3656(3)	4430(2)
<i>Z</i>	4	8	4	4	8
Density (calc.) Mg m ⁻³	1.838	1.579	1.245	1.677	1.481
μ /mm ⁻¹	5.452	3.889	0.072	3.904	0.904 mm ⁻¹
<i>F</i> (000)	1352	3384	760	1828	2032
Crystal size mm	0.20 × 0.17 × 0.06	0.39 × 0.09 × 0.09	0.19 × 0.13 × 0.05	0.26 × 0.17 × 0.08	0.24 × 0.07 × 0.03
Theta range	1.48 to 27.00	1.36 to 27.00	1.83 to 25.00	1.69 to 26.00	1.72 to 26.00
Index ranges	-11 ≤ <i>h</i> ≤ 11, -35 ≤ <i>k</i> ≤ 34, -14 ≤ <i>l</i> ≤ 14	-27 ≤ <i>h</i> ≤ 27, -27 ≤ <i>k</i> ≤ 26, -20 ≤ <i>l</i> ≤ 20	-12 ≤ <i>h</i> ≤ 12, -9 ≤ <i>k</i> ≤ 9, -27 ≤ <i>l</i> ≤ 27	-14 ≤ <i>h</i> ≤ 14, -17 ≤ <i>k</i> ≤ 17, -25 ≤ <i>l</i> ≤ 26	-16 ≤ <i>h</i> ≤ 16, -17 ≤ <i>k</i> ≤ 17, -29 ≤ <i>l</i> ≤ 28
Reflections collected	21132	60010	13317	27890	32847
Independent reflections (<i>R</i> _{int})	5464 [<i>R</i> _{int} = 0.0290]	7840 [<i>R</i> _{int} = 0.0796]	3379 [<i>R</i> _{int} = 0.1222]	7169 [<i>R</i> _{int} = 0.0638]	4347 [<i>R</i> _{int} = 0.2825]
Data/restraints/parameters	5464/0/376	7840/0/398	3379/0/254	7169/0/448	4347/0/268
Goodness-of-fit, <i>F</i> ²	0.999	0.804	0.870	0.974	0.934
Final <i>R</i> indices [<i>I</i> > 2σ(<i>I</i>)]	<i>R</i> ₁ = 0.0230, <i>wR</i> ₂ = 0.0551	<i>R</i> ₁ = 0.0403, <i>wR</i> ₂ = 0.0691	<i>R</i> ₁ = 0.0654, <i>wR</i> ₂ = 0.1331	<i>R</i> ₁ = 0.0340, <i>wR</i> ₂ = 0.0773	<i>R</i> ₁ = 0.0723, <i>wR</i> ₂ = 0.1073
<i>R</i> indices (all data)	<i>R</i> ₁ = 0.0269, <i>wR</i> ₂ = 0.0563	<i>R</i> ₁ = 0.0727, <i>wR</i> ₂ = 0.0756	<i>R</i> ₁ = 0.1560, <i>wR</i> ₂ = 0.1649	<i>R</i> ₁ = 0.0439, <i>wR</i> ₂ = 0.0817	<i>R</i> ₁ = 0.1518, <i>wR</i> ₂ = 0.1266
Largest diff. peak and hole/e Å ⁻³	0.995 and -0.501	1.030 and -0.412	0.376 and -0.198	1.407 and -0.861	0.806 and -1.307

150 K. The data were corrected for Lorentz and polarisation effects and empirical absorption corrections (SADABS).²⁸ were applied in all cases. The structures were solved by Patterson methods and refined by full-matrix least squares on F^2 using the program SHELXTL.²⁹ All hydrogen atoms bonded to carbon were included in calculated positions (C–H = 0.96 Å) using a riding model. All non-hydrogen atoms were refined with anisotropic displacement parameters without positional restraints. Figures were drawn using the program ORTEP.³⁰

Acknowledgements

We thank the Saudi Arabian government (O. A-D) for a studentship, the EPSRC for financial support (YB), Professor S. A. Macgregor (Heriot Watt) for discussions, and Johnson Matthey for a loan of platinum metal salts.

References

- 1 For general reviews of cyclometallated complexes see: M. Ghedini, I. Aiello, A. Crispini, A. Golemme, M. La Deda and D. Pucci, *Coord. Chem. Rev.*, 2006, **250**, 1373–1390; V. Ritleng, C. Sirlin and M. Pfeffer, *Chem. Rev.*, 2002, **102**, 1731–1769; R. B. Bedford, *Chem. Commun.*, 2003, 1787–1796; J. Dupont, M. Pfeffer and J. Spencer, *Eur. J. Inorg. Chem.*, 2001, 1917–1927; J. Dupont, C. S. Consorti and J. Spencer, *Chem. Rev.*, 2005, **105**, 2527–2571; M. Albrecht, *Chem. Rev.*, 2010, **110**, 576–623; J. P. Djukic, J. B. Sortais, L. Barloy and M. Pfeffer, *Eur. J. Inorg. Chem.*, 2009, 817–853.
- 2 D. L. Davies, O. Al-Duaij, J. Fawcett, M. Giardiello, S. T. Hilton and D. R. Russell, *Dalton Trans.*, 2003, 4132–4138.
- 3 D. L. Davies, S. M. A. Donald, O. Al-Duaij, S. A. Macgregor and M. Polleth, *J. Am. Chem. Soc.*, 2006, **128**, 4210–4211; Y. Boutadla, D. L. Davies, S. A. Macgregor and A. I. Poblador-Bahamonde, *Dalton Trans.*, 2009, 5887–5893.
- 4 L. Li, W. W. Brennessel and W. D. Jones, *Organometallics*, 2009, **28**, 3492–3500.
- 5 Y. Boutadla, D. L. Davies, S. A. Macgregor and A. I. Poblador-Bahamonde, *Dalton Trans.*, 2009, 5820–5831.
- 6 Y. Boutadla, O. Al-Duaij, D. L. Davies, G. A. Griffith and K. Singh, *Organometallics*, 2009, **28**, 433–440; J. F. Hull, D. Balcells, J. D. Blakemore, C. D. Incarvito, O. Eisenstein, G. W. Brudvig and R. H. Crabtree, *J. Am. Chem. Soc.*, 2009, **131**, 8730–8731; Y.-K. Sau, X.-Y. Yi, K.-W. Chan, C.-S. Lai, I. D. Williams and W.-H. Leung, *J. Organomet. Chem.*, 2010, **695**, 1399–1404.
- 7 L. Li, W. W. Brennessel and W. D. Jones, *J. Am. Chem. Soc.*, 2008, **130**, 12414–12419.
- 8 C. Scheeren, F. Maassarani, A. Hijazi, J. P. Djukic, M. Pfeffer, S. D. Zaric, X. F. LeGoff and L. Ricard, *Organometallics*, 2007, **26**, 3336–3345.
- 9 For reviews of catalytic reactions involving C–H activation see: F. Kakiuchi and S. Murai, *Acc. Chem. Res.*, 2002, **35**, 826–834; D. Alberico, M. E. Scott and M. Lautens, *Chem. Rev.*, 2007, **107**, 174–238; L. Ackermann, A. Althammer and R. Born, *Tetrahedron*, 2008, **64**, 6115–6124; S. Oi, R. Funayama, T. Hattori and Y. Inoue, *Tetrahedron*, 2008, **64**, 6051–6059; F. Kakiuchi and T. Kochi, *Synthesis*, 2008, 3013–3039; J. C. Lewis, R. G. Bergman and J. A. Ellman, *Acc. Chem. Res.*, 2008, **41**, 1013–1025; T. Satoh and M. Miura, *Chem. Lett.*, 2007, **36**, 200–205; G. Dyker, ed., *Handbook of C–H transformations*, Wiley-VCH, Weinheim, 2005.
- 10 T. Fukutani, N. Umeda, K. Hirano, T. Satoh and M. Miura, *Chem. Commun.*, 2009, 5141–5143.
- 11 K. Kokubo, K. Matsumasa, Y. Nishinaka, M. Miura and M. Nomura, *Bull. Chem. Soc. Jpn.*, 1999, **72**, 303–311; S. Mochida, K. Hirano, T. Satoh and M. Miura, *J. Org. Chem.*, 2009, **74**, 6295–6298; M. Shimizu, K. Hirano, T. Satoh and M. Miura, *J. Org. Chem.*, 2009, **74**, 3478–3483; M. Shimizu, H. Tsurugi, T. Satoh and M. Miura, *Chem.–Asian J.*, 2008, **3**, 881–886; K. Ueura, T. Satoh and M. Miura, *Org. Lett.*, 2007, **9**, 1407–1409; K. Ueura, T. Satoh and M. Miura, *J. Org. Chem.*, 2007, **72**, 5362–5367.
- 12 N. Umeda, H. Tsurugi, T. Satoh and M. Miura, *Angew. Chem., Int. Ed.*, 2008, **47**, 4019–4022.
- 13 D. R. Stuart, M. Bertrand-Laperle, K. M. N. Burgess and K. Fagnou, *J. Am. Chem. Soc.*, 2008, **130**, 16474–16475.
- 14 N. Guimond and K. Fagnou, *J. Am. Chem. Soc.*, 2009, **131**, 12050–12051.
- 15 M. Pfeffer, J. P. Sutter and E. P. Urriolabeitia, *Bull. Soc. Chim. Fr.*, 1997, **134**, 947–954; H. C. L. Abbenhuis, M. Pfeffer, J.-P. Sutter, A. de Cian, J. Fischer, H. L. Ji and J. H. Nelson, *Organometallics*, 1993, **12**, 4464–4472; W. Ferstl, I. K. Sakodinskaya, N. Beydoun-Sutter, G. LeBorgne, M. Pfeffer and A. D. Ryabov, *Organometallics*, 1997, **16**, 411–418.
- 16 D. L. Davies, O. Al-Duaij, J. Fawcett and K. Singh, *Organometallics*, 2010, **29**, 1413–1420.
- 17 Y. Boutadla, D. L. Davies, and K. Singh, personal communication.
- 18 D. L. Davies, J. Fawcett, S. A. Garratt and D. R. Russell, *Organometallics*, 2001, **20**, 3029–3034.
- 19 R. P. Korivi and C.-H. Cheng, *Org. Lett.*, 2005, **7**, 5179–5182; R. P. Korivi, Y.-C. Wu and C.-H. Cheng, *Chem.–Eur. J.*, 2009, **15**, 10727–10731; K. Cheng, B. Yao, J. Zhao and Y. Zhang, *Org. Lett.*, 2008, **10**, 5309–5312; L. Chuan-Che, K. Rajendra Prasad and C. Chien-Hong, *Chem.–Eur. J.*, 2008, **14**, 9503–9506.
- 20 M. R. Meneghetti, M. Grellier, M. Pfeffer and J. Fischer, *Organometallics*, 2000, **19**, 1935–1939.
- 21 F. Maassarani, M. Pfeffer and G. Leborgne, *Organometallics*, 1987, **6**, 2029–2043; F. Maassarani, M. Pfeffer and G. Leborgne, *J. Chem. Soc., Chem. Commun.*, 1987, 565–567.
- 22 G. Wu, A. L. Rheingold, S. J. Geib and R. F. Heck, *Organometallics*, 1987, **6**, 1941–1946.
- 23 D. L. Davies, O. Al-Duaij, J. Fawcett and K. Singh, *J. Organomet. Chem.*, 2008, **693**, 965–980.
- 24 We can't rule out C,C bond formation to make an indene, however, all other examples of this feature are an NPh imine.
- 25 D. L. Davies, S. A. Macgregor, and A. Poblador-Bahamonde, personal communication.
- 26 C. White, A. Yates and P. M. Maitlis, *Inorg. Synth.*, 1992, **29**, 228.
- 27 M. A. Bennett and A. K. Smith, *J. Chem. Soc., Dalton Trans.*, 1974, 233.
- 28 Bruker, Bruker Inc., Madison, Wisconsin, USA, Version 6.02 edn, 1998–2000.
- 29 Bruker, Bruker Inc, Madison, Wisconsin, USA, Version 6.10 edn, 1998–2000.
- 30 L. J. Farrugia, *J. Appl. Crystallogr.*, 1997, **30**, 565.